Available online at www.sciencedirect.com
SCIENCE DIRECT®
Bioorganic & Medicinal Chemistry 13 (2005) 4243–4252
Bioorganic & Medicinal Chemistry

5-Arylidene-2-imino-4-thiazolidinones: Design and synthesis of novel anti-inflammatory agents

Rosaria Ottanà,[a,*] Rosanna Maccari,[a] Maria Letizia Barreca,[a] Giuseppe Bruno,[b] Archimede Rotondo,[b] Antonietta Rossi,[c] Giuseppa Chiricosta,[a] Rosanna Di Paola,[d] Lidia Sautebin,[c] Salvatore Cuzzocrea[d] and Maria Gabriella Vigorita[a]

[a]*Dipartimento Farmaco-chimico, Facoltà di Farmacia, Università di Messina, Viale SS. Annunziata, 98168 Messina, Italy*
[b]*Dipartimento Ch. Inorg., Chim. Anal. e Ch.-fis., Facoltà di Scienze MMFFNN, Università di Messina, Salita Sperone, 31, 98166 Messina, Italy*
[c]*Dipartimento di Farmacologia Sperimentale, Universitá di Napoli 'Federico II', Via Domenico Montesano 49, 80131 Napoli, Italy*
[d]*Istituto di Farmacologia, Facoltà di Medicina e Chirurgia, Università di Messina, Policlinico Universitario 'G. Martino', Via Consolare Valeria, 98124 Messina, Italy*

Received 1 July 2004; accepted 12 April 2005
Available online 17 May 2005

Abstract—The synthesis and pharmacological activity of 5-arylidene-2-imino-4-thiazolidinones (**3a**–**8a**) are described. All derivatives exhibited significant activity levels in models of acute inflammation such as carrageenan-induced paw and pleurisy edema in rats. In particular, 5-(3-methoxyphenylidene)-2-phenylimino-3-propyl-4-thiazolidinone (**3a**) displayed high levels of carrageenan-induced paw edema inhibition comparable to those of indomethacin. In addition the ability of such a new class of anti-inflammatory agents to inhibit COX isoforms was assessed in murine monocyte/macrophage J774 cell line assay. 5-(4-Methoxyphenylidene)-2-phenylimino-3-propyl-4-thiazolidinone (**6a**), the most interesting compound in such an experiment, was docked in the known active site of COX-2 protein and showed that its 4-methoxyarylidene moiety can easily occupy the COX-2 secondary pocket considered as the critical interaction for COX-2 selectivity.

1. Introduction

Nonsteroidal anti-inflammatory drugs (NSAIDs) are an unhomogeneous family of pharmacologically active compounds used in the treatment of acute and chronic inflammation, pain, and fever. However, nevertheless NSAIDs are the most widely used drugs, their long-term clinical employment is associated with significant side effects and the steady use determines the onset of gastrointestinal lesions, bleeding, and nephrotoxicity.[1,2]

Therefore the discovery of new safer anti-inflammatory drugs represents a challenging goal for such a research area.

Although several mediators support the inflammatory processes, the main target of NSAIDs is cyclooxygenase (COX),[3] the enzyme involved in the first step of the conversion of arachidonic acid to prostaglandins (PGs). These latter regulate important functions in the gastric, renal, and ematic systems and are known to mediate all inflammatory responses. Classical NSAIDs, such as indomethacin, inhibit both isoforms of COX:[4] COX-1, which is constitutively expressed in most tissues and organs and catalyzes the synthesis of PGs involved in the regulation of physiological cellular activities; COX-2, which is mainly induced by several stimuli such as cytokines, mitogens, and endotoxins in inflammatory sites.[5–7] Thus, their therapeutical effects are mainly due to the decrease of proinflammatory PGs produced by COX-2, whereas their unwanted side effects result from the inhibition of constitutive COX-1 isoform.

Recently highly selective COX-2 inhibitors belonging to the classes of diarylheterocycles and methanesulfonanilides have been developed and marketed.[8] In particular the class of Coxibs is characterized by 1,2-diaryl substituted heterocycles often bearing a sulfonyl moiety at the

* Corresponding author. Tel.: +33 90 6766408; fax: +39 90 355613; e-mail: ottana@pharma.unime.it

0968-0896/$ - see front matter © 2005 Elsevier Ltd. All rights reserved.
doi:10.1016/j.bmc.2005.04.058

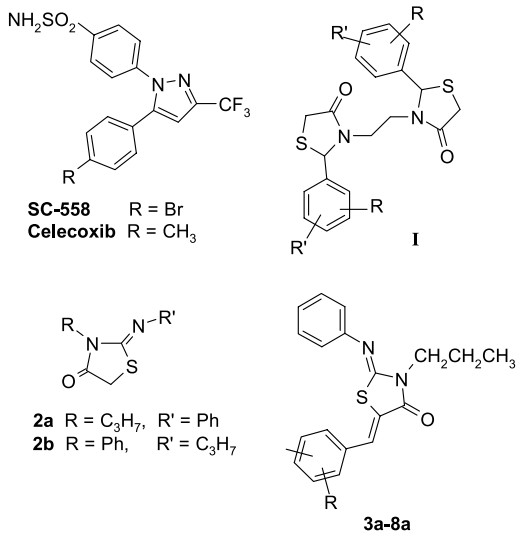

Figure 1.

para-position of one of the aryl rings, for example, celecoxib (Celebrex®) (Fig. 1).[9]

Some of us had long investigated 3,3′-(1,2-ethanediyl)-bis[2-aryl-4-thiazolidinone] derivatives (**I**, Fig. 1), which showed interesting stereoselective anti-inflammatory/analgesic activities together with better gastrointestinal safety profile than known NSAIDs,[10] suggesting they might preferentially interact with inducible COX-2 isoform. Suitable selectivity assays as well as molecular modeling studies had supported this hypothesis.[10e]

Within this context we were then stimulated to similarly explore simplified 4-thiazolidinone analogues in order to find the pharmacophore of the class. Therefore, we synthesized 2-imino-4-thiazolidinones **2a**, **2b**, and 5-arylidene-2-imino-4-thiazolidinones **3a**–**8a**. These latter 1, 3-diaryl substituted derivatives can be considered diarylheterocycle Coxib-like compounds (Fig. 1). The effect of Cl, OCH_3, SCH_3, and SO_2CH_3 substituents of the arylidene moiety on the anti-inflammatory profile was considered. These substituents were selected on the basis of previous SAR studies on bisthiazolidinones, also keeping in mind the most frequent substituents in Coxibs structures.

The novel 4-thiazolidinones were tested for in vivo anti-inflammatory activity by carrageenan-induced paw edema and pleurisy assays in rats.[11,12] With the aim of investigating their possible action mechanism, their ability to inhibit COX-1 and COX-2 was assessed in murine monocyte/macrophage J774 cell line.[13] Finally the most promising among the tested compounds (**6a**) was docked into the active site of COX-2 enzyme in comparison with the known selective COX-2 inhibitor SC-558 (Fig. 1).[14]

2. Chemistry

Compounds **2** and **3a**–**8a** were synthesized according to the synthetic pathway described in Schemes 1 and 3. The

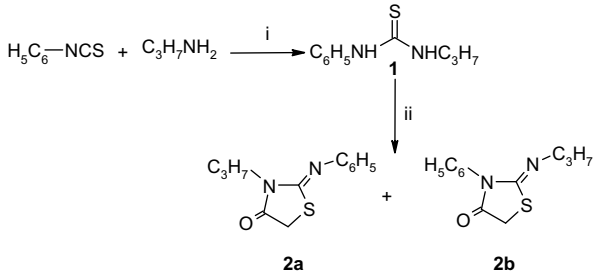

Scheme 1. Reagents and conditions: (i) Et_3N, $CHCl_3$, rt, 4 h; (ii) $ClCH_2COCl$, Et_3N, $CHCl_3$, rt, 12 h.

starting product was *N*-propyl-*N*′-phenylthiourea (**1**) obtained by the reaction of propylamine and phenylisothiocyanate in $CHCl_3$ at room temperature for 4 h followed by work-up under acidic conditions (Scheme 1).

Subsequent synthesis of 2-imino-4-thiazolidinones **2** was performed by condensation of thiourea **1** with chloroacetyl chloride in the presence of triethylamine in $CHCl_3$ at room temperature. The reaction provided a mixture of two isomers arylimino **2a** and propylimino **2b** in about 1:2 ratio. They conceivably originated from the condensation of chloroacetyl chloride with the sulfur atom of two different intermediate thiols generated from **1** by delocalization of the lone pairs of the two different nitrogens on the adjacent thiocarbonyl group. The synthesis of isomer **2b** was favored by the intermediate thiol involving the NH group adjacent to the electron releasing group. However, the nature of solvent proved to be determinant for the reaction course. In fact, when the synthesis was performed in MeOH at reflux, **2a**/**2b** ratio changed depending on the reaction time: after 24 h the most stable isomer (**2a**) was the only product.

The suggested mechanism of the conversion of **2b** into **2a** is depicted in Scheme 2. The extended electronic delocalization of amidine system gave rise to the cleavage of the cyclic amide bond. A possible low barrier around the C–S σ bond and the subsequent cyclization accounted for the intramolecular rearrangement providing the most stable arylimino isomer (**2a**).

The structure of isomers **2a** and **2b** was assessed by elemental analysis and ^1H and ^{13}C NMR. The resonances of propyl protons allowed us to identify each isomer. In **2a** the $CH_2CH_2CH_3$ protons appeared as a triplet resonating to higher chemical shift (3.82 ppm) than the same protons of **2b** (3.27 ppm) due to the higher deshiel-

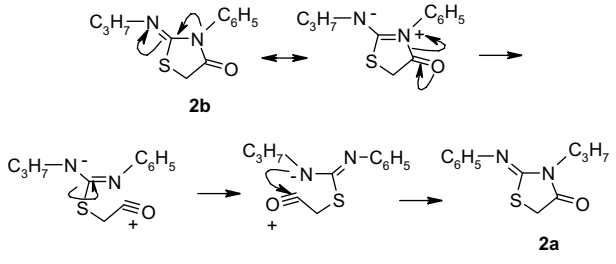

Scheme 2. Rearrangement of **2b** into **2a**.

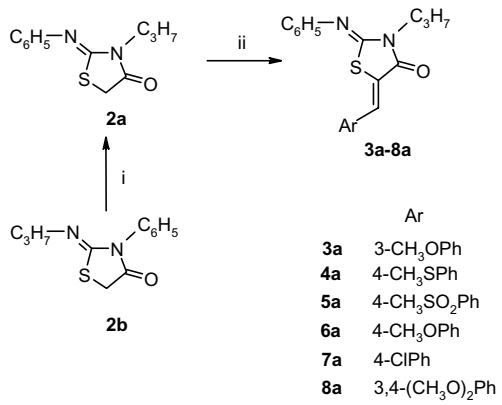

Scheme 3. Reagents and conditions: (i) EtOH, reflux, 24 h; (ii) ArCHO, piperidine, EtOH, reflux, 24 h.

ding effect generated by the extended electronic delocalization of 3-N lone pair.

5-Arylidene-2-imino-4-thiazolidinones were synthesized by the reaction in basic conditions of compounds **2** and appropriate aldehydes in refluxing ethanol for about 24 h.[15] In such experimental conditions derivatives **3a**–**8a** were obtained starting from pure compounds **2a**, **2b** as well as from any mixture of them.

Moreover, the synthesis of **3a** from **2b** was monitored by ^{1}H NMR spectra of successive samples taken from the reaction mixture. Starting from **2b** spectrum, new sets of signals attributable to isomer **2a** appeared after 6 h, which progressively increased. The conversion into **3a** was completed after 24 h (Scheme 3).

The structures of 5-arylidene derivatives (**3a**–**8a**) were assigned on the basis of analytical and spectral data. In their ^{1}H NMR spectra, the absence of the signal of 5-CH_2 protons of starting compounds **2** at 3.80 ppm together with the resonance of the methine hydrogen (7.70–7.75 ppm) agreed with the proposed structures. Moreover ^{13}C spectra showed clear changes in splitting pattern of 5-C, which resonated as a triplet in **2** and as a singlet in compounds **3a**–**8a**.

The *Z* configuration of the exocyclic C=C bond was assigned on the basis of ^{1}H NMR spectroscopy and X-ray crystallography results. The methine proton, deshielded by the adjacent C=O, was detected at 7.70–7.75 ppm in ^{1}H NMR spectra as observed for analogous 5-arylidene-2,4-thiazolidinediones.[16] In *E* isomers, due to the lesser deshielding effect of 1-S, such a proton should resonate at lower chemical shift values.[15]

Furthermore, the X-ray diffractometric analysis of a representative compound (**6a**) unambiguously confirmed the *Z* configuration at the chiral axis (Fig. 2).

3. Results and discussion

Compounds **3a**–**8a**, representative of the class of 5-arylidene-2-phenylimino-4-thiazolidinones, and their precursors **2a**, **2b** were explored to evaluate their anti-inflammatory activity by carrageenan-induced rat paw and pleurisy edema assays.[11,12] Indomethacin and celecoxib were used as reference drugs.

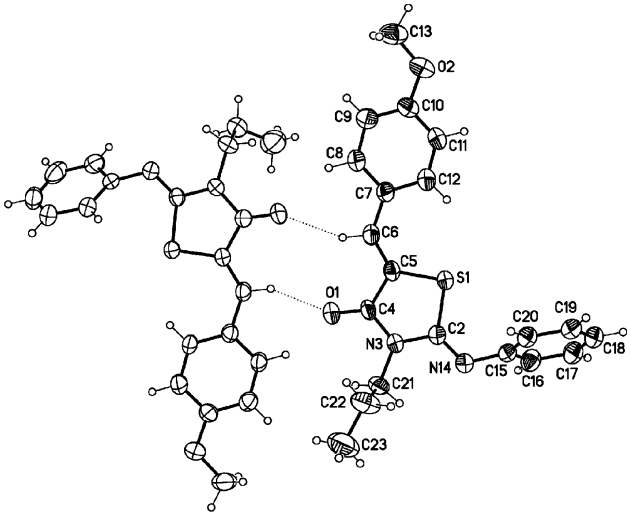

Figure 2. X-ray structure of **6a**.

Compounds **2b** and **2a**–**7a** proved to have interesting in vivo activities in both animal models; on the contrary **8a** was devoid of any ability to inhibit the inflammation process in such assays.

The injection of carrageenan into the rat paw produced a marked increase of volume from the first hour, reaching its maximal effect after 3–4 h. Pretreatment of rats with tested compounds, except **8a**, administered (10 mg/kg, intraperitoneally) 30 min before the carrageenan injection, significantly attenuated inflammatory response (Fig. 3).

The 3-methoxyarylidene derivative (**3a**) proved to be the most effective compound, achieving an inhibition level (85% at the third hour) similar to that of indomethacin, while it showed a better activity profile than celecoxib,[17] which reached 38% edema inhibition at the same hour

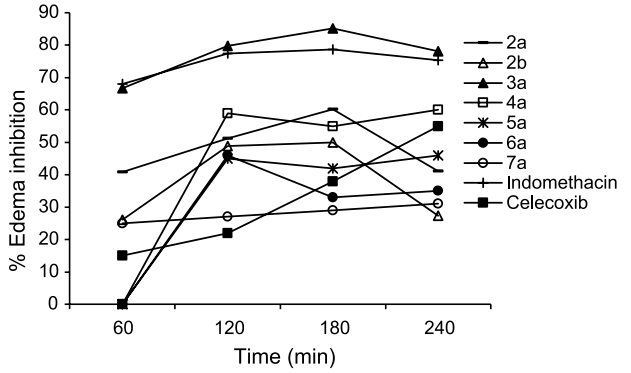

Figure 3. Effect of 5-arylidene-2-imino-4-thiazolidinones on rat paw edema development elicited by carrageenan in the rat. Data are means of mean ± SEM from $n = 10$ rats for each group.

(Fig. 3). By moving the methoxy group to the *para*-position (**6a**) the activity decreased: in fact, the edema inhibition at most reached 46% at the second hour.

In addition, 4-substituted analogues **4a**–**6a**, inactive at the first hour, proved to inhibit paw edema from the second to the fourth hour after carrageenan administration. Moreover, a comparison between derivatives **4a** (4-SCH_3 substituted) and **5a** (4-SO_2CH_3) indicated the sulfur oxidation was slightly detrimental to the anti-inflammatory activity (Fig. 3). The 4-chloroarylidene analogue (**7a**) was shown to be less active (20–30% inhibition) than the other 4-substituted derivatives.

Such preliminary findings stimulated us to carry out the carrageenan-induced pleurisy assay that could provide additional information. In this model all carrageenan-injected rats developed an acute pleurisy producing turbid exudates (Fig. 4) that contained a large amount of polymorphonuclear cells (PMNs) (Fig. 5). Neutrophils, measured as myeloperoxidase activity, also infiltrated the lung tissue (Fig. 6). Sham animals demonstrated no abnormalities in the pleural cavity or fluid.

Pretreatment of rats with all compounds (20 mg/kg, i.p.), except **8a**, significantly reduced the degree of lung injury as well as PMNs infiltration (Figs. 4 and 5). In particular, compounds **4a**–**6a** showed effectiveness similar to those of indomethacin and celecoxib in reducing exudate volume and PMNs infiltration. Besides, the myeloperoxidase inhibitory effects of **5a**, **4a**, **3a**, and **2b** were greater than those of the reference drugs (Fig. 6).

In addition the levels of PGE_2 in pleural exudates, which are considered as a measurement of the COX-2 activity,[12] were assessed (Fig. 7).

Compounds **3a**, **4a**, and **6a** significantly reduced PGE_2 levels without reaching the level of effectiveness of celecoxib. On the contrary **5a**, which showed the best anti-inflammatory profile in the pleurisy model, did not reduce PGE_2 level in pleural exudates.

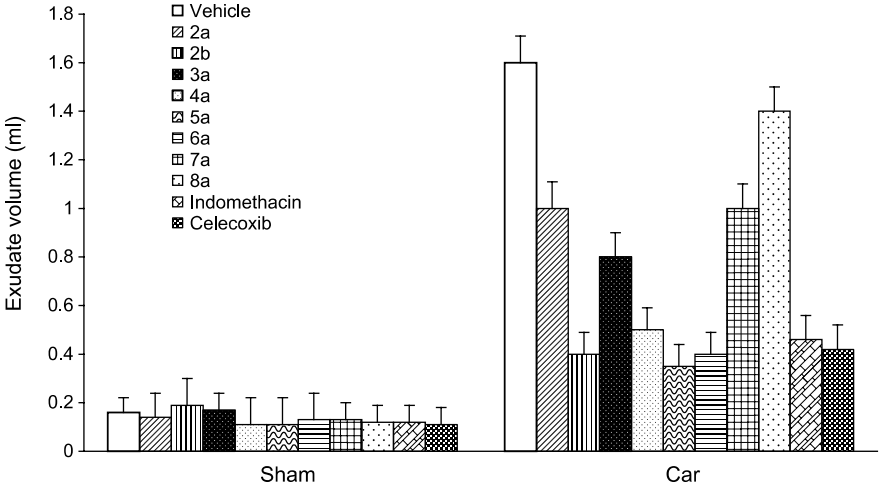

Figure 4. Effect of 5-arylidene-2-imino-4-thiazolidinones on carrageenan-induced pleurisy assay. Exudate volume in pleural cavity at 4 h after carrageenan injection. Data are means of mean ± SEM from $n = 10$ rats for each group.

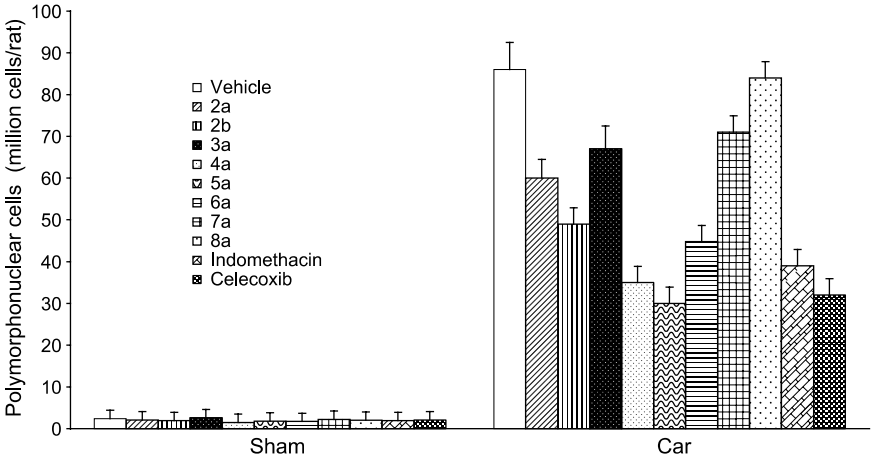

Figure 5. Effect of 5-arylidene-2-imino-4-thiazolidinones on carrageenan-induced accumulation of polymorphonuclear cells in pleural cavity at 4 h after carrageenan injection. Data are means of mean ± SEM from $n = 10$ rats for each group.

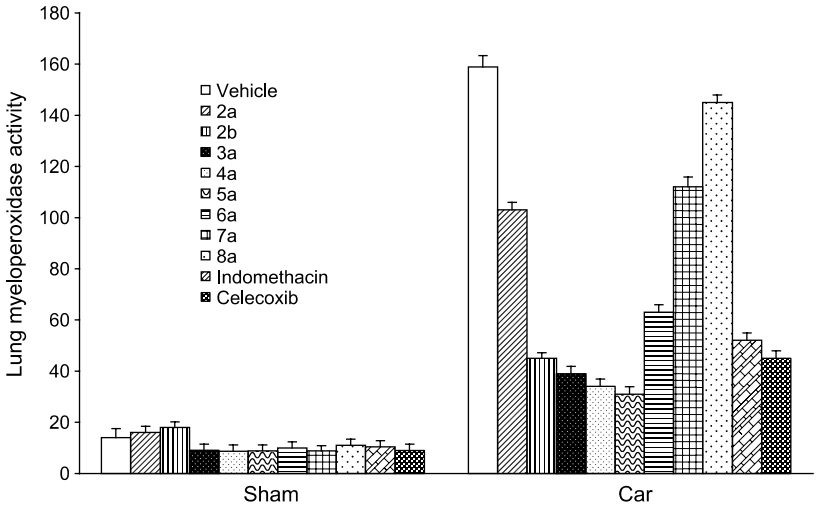

Figure 6. Effect of 5-arylidene-2-imino-4-thiazolidinones on myeloperoxidase activity in the lung of carrageenan-treated rats sacrificed after 4 h after carrageenan injection. Lung myeloperoxidase activity is expressed as mU/100 mg wet tissue. Data are means of mean ± SEM from $n = 10$ rats for each group.

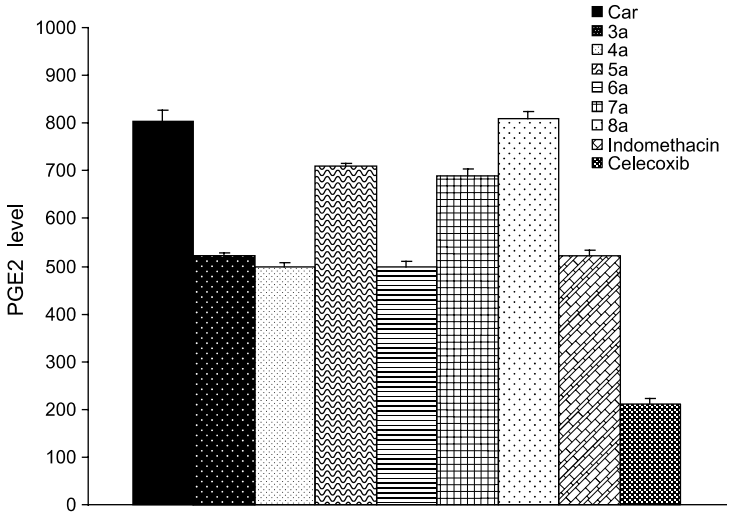

Figure 7. Effect of 5-arylidene-2-imino-4-thiazolidinones on PGE_2 levels in the pleural exudate from carrageenan-treated rats. PGE_2 exudate levels are expressed as pg/rat. Data are means ± SEM of 10 rats for each group.

In order to clarify whether such results were related to the COX-1/COX-2 inhibition, in vitro assays were performed in murine macrophage J774 cell line (Table 1)[13] at concentrations not higher than 10 μM because of their low solubility in the culture media.

In this assay compounds **2a** and **2b** produced only a weak inhibition of COX-1 isoform at all tested doses, without inhibiting COX-2.

The introduction of a (*Z*)-5-arylidene group generally gave rise to the inhibition of COX-2 while the potency increased without reaching, however, the levels of the reference drugs. In particular, the insertion of a substituent at the *para*-position of the arylmethylidene group appeared to be useful for COX-2 inhibition, except for **5a**. In fact, the compound bearing the 4-OCH_3 group (**6a**) showed higher COX-2 inhibitory potency than the 3-substituted analogue (**3a**) at the same concentration. Isosteric replacement of the oxygen atom with sulfur resulted in compound **4a**, which displayed irrelevant differences in inhibitory potency and selectivity with respect to **6a**. Surprisingly, the oxidation of SCH_3 group (**4a**) led to a selective COX-1 inhibitor (**5a**), contrary to what takes place in well-known selective COX-2 inhibitors.[8] These in vitro results suggested that compounds displaying COX-2 inhibitory activity also produced appreciable reduction of PGE_2 levels in pleural exudates (Fig. 7).

The replacement of the 4-methoxy substituent with an electron-withdrawing group, such as chlorine, afforded compound **7a**, which showed a profile comparable to that of the parent analogue (**6a**). The coexistence of two methoxy groups in meta- and para-positions of

Table 1. In vitro assays for inhibition of COX-1 and COX-2

Compd	Concn (μM)	COX-1[a] (%)	COX-2[a] (%)	Compd	Concn (μM)	COX-1[a] (%)	COX-2[a] (%)
2a	0.1	2	0	**5a**	0.1	23	3
	1	10	0		1	42	11
	10	12	0		10	51	13
2b	0.1	1	0	**6a**	0.1	0	16
	1	5	0		1	0	35
	10	8	0		10	0	55
3a	0.1	0	5	**7a**	0.1	0	20
	1	0	13		1	0	30
	10	0	24		10	0	55
4a	0.1	0	10	**8a**	0.1	0	6
	1	0	25		1	0	10
	10	0	42		10	0	22
Celecoxib	0.1	4	61	Indomethacin	0.1	37	43
	1	31	73		1	40	63
	10	62	93		10	58	69

[a] Percentage COX-1 and COX-2 inhibition in murine monocyte/macrophage J774 cells at the reported doses ($n = 5$). Assays were repeated so that standard errors were less than 5%.

the arylidene moiety (**8a**) was also shown to be detrimental for in vitro activity.

4. Binding orientation in the COX-2 active site

Using as macromolecule target the X-ray structure of the enzyme from SC-558/COX-2 complex,[14] computational docking simulations were performed to explore the binding mode of this new class of anti-inflammatory drug. The software used for our calculations was AutoDock 3.0[18] and all ligand atoms but no protein atoms were allowed to move during the calculations.[19]

To validate the docking protocol, the ligand conformation of SC-558 was extracted from the crystal structure of the corresponding COX-2/ligand complex and later docked back into the binding pocket. AutoDock was able to perfectly reproduce the experimental position of the ligand (62 runs of 100, with a binding free energy of −12.09 kcal/mol), confirming the ability of the method to accurately predict the binding conformation.

Then, the most active COX-2 inhibitor of the series, compound **6a**, was chosen for our docking experiments. Compound **6a** clearly preferred a single binding position in the typical binding pocket (channel-site) of COX-2 (48 runs of 100, with a binding free energy of −11.74 kcal/mol), which was the best prediction since it had the lowest energy among the clusters. Comparison of the experimental position of SC-558 with **6a** showed that the following parts of these molecules are perfectly overlapped: the methoxyphenyl, the 3-phenylimino, and the propyl groups of 2-imino-4-thiazolidinone system of **6a** are superimposed to the phenyl sulfonamide and 4-bromophenyl moieties and to the trifluoromethyl group of SC-558, respectively (Fig. 8).

In such orientation, the bound conformation of **6a** was engaged in hydrogen-bonds with Arg 120 and Tyr 355 and was involved in van der Waals contacts with the

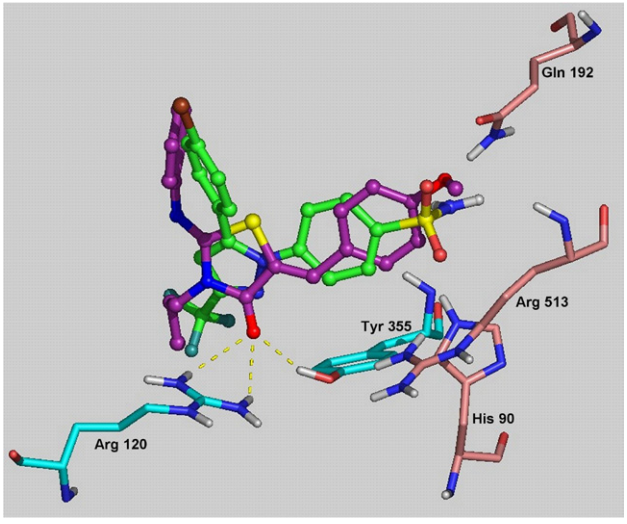

Figure 8. AutoDock-predicted binding mode of the ligand **6a** (purple) compared to the crystallized position of SC-558 (green). Residues of the binding site with important contacts to the ligands are shown, while yellow dashed lines indicate hydrogen bonds.[24]

residues of the binding pocket, that is, His 90, Val 349, Leu 352, Ser 353, Leu 359, Tyr 385, Ala 516, Phe 518, Val 523, Gly 526, Ala 527, Ser 530, and Leu 531.[14]

Previous studies had shown that the COX-2 binding site was 25% larger than the COX-1 due to the substitution of a single amino acid (valine for isoleucine at position 523), so originating a secondary internal pocket not accessible in COX- 1.[20]

Authors suggested that the selectivity of SC-558 for COX-2 over COX-1 might result from additional contacts with residues along this deeper binding region. In fact, the structural analysis of SC-558/COX-2 complex indicated that the selective inhibitor molecule interacted with His 90, Gln 192, and Arg 513, which are located at the bottom of the COX-2 gorge. It is worth noting that

compound **6a** was able to reach such a gorge rationalizing the COX-2 selectivity (Fig. 8).

5. Conclusions

We report on a novel series of 5-arylidene-2-imino-4-thiazolidinones designed as simplified analogues of previously reported anti-inflammatory bisthiazolidinones (**I**)[10] and, at the same time, as Coxib-like compounds. They generally retained the in vivo activity already showed by the bisthiazolidinone class and could be a novel class of anti-inflammatory agents. Although a wide SAR picture is not yet available, some considerations can be focused. The attempt to simplify the parent structure (**I**) and identify its pharmacophoric part initially led to compounds **2**, which retained good anti-inflammatory profiles when a differently substituted arylidene moiety was inserted in position 5 (**3a**–**8a**). In particular: (a) the OCH_3, SCH_3, and SO_2CH_3 groups introduced in the para-position of the arylidene moiety were generally found to be favorable for activity both in vivo and in vitro experiments; (b) in addition, while the introduction of the SO_2CH_3 group generally leads to COX-2 selective inhibitors, in the compounds herein reported such a moiety proved to be a determinant of COX-1 inhibition; (c) the 4-Cl substitution decreased the in vivo anti-inflammatory activity while the degree of selective COX-2 inhibition was retained; (d) when the OCH_3 substituent moved to position 3 (**3a**), a good in vivo anti-inflammatory profile was achieved, reaching indomethacin levels in the carrageenan-induced rat paw edema, without displaying any preference for each one of the COX isoforms; (e) when steric hindrance increased (**8a**), both in vitro and in vivo activities disappeared; (f) flexible docking experiments showed that **6a** and SC-558 have a similar binding mode to the COX-2 active site with good overlapping.

The observed COX inhibition did not appear to be the only action mode of this class of anti-inflammatory agents. This is not surprising since inflammation is a complex physiopathological reaction and several mediators are involved in its development and progression. Consequently further investigations will be performed in order to clarify the anti-inflammatory mechanism of action of these compounds.

6. Experimental

6.1. Chemistry

Melting points were determined with a Kofler–Reichert hot-stage apparatus and are uncorrected. Precoated silica gel plates F 254 for analytical controls and chromatographic columns 70–230 mesh SiO_2 for separations were used. Elemental analyses (C, H, N), determined by means of a C. Erba mod. 1106 elem. analyzer, were within ±0.4% of theory. IR spectra were registered as Nujol mulls on a Perkin Elmer mod. 683 Spectrophotometer. The NMR spectra were obtained on a Varian 300 magnetic resonance spectrometer (300 MHz for ^1H and 75 MHz for ^{13}C) with deuterochloroform as solvent and internal standard unless otherwise indicated. The chemical shifts are given in δ values and the coupling constants (J) in hertz (Hz).

Unless stated otherwise, all materials were obtained from commercial suppliers and used without further purification.

Crystals suitable for X-ray analysis were obtained by recrystallization of compound **6a** from methanol solution. Diffraction data were collected at room temperature from a colorless $0.92 \times 0.75 \times 0.36\ mm^3$ prismatic crystal sample by using a Siemens P4 automated four-cycle single-crystal diffractometer with graphite-monochromated MoK_α radiation ($\lambda = 0.71073$ Å). Crystallographic data (excluding structure factors) for compound **6a** have been deposited with the Cambridge Crystallographic Data Centre as supplementary publication no. CCDC 216008. Copies of the data can be obtained, free of charge, on application to CCDC, 12 Union Road, Cambridge CB2 1EZ, UK (fax: +44-1223-336033; e-mail: deposit@ccdc.cam.ac.uk).

6.2. Synthesis of *N*-phenyl-*N*′-propylthiourea (1)

Propylamine (0.65 g, 0.011 mol) was added to a solution of phenylisothiocyanate (1.53 g, 0.01 mol) dissolved in chloroform (30 mL). The solid was stirred for about 4 h at room temperature and concentrated under reduced pressure. The precipitate was filtered and crystallized from cold ethanol to give 1.69 g (87%) of the title compound as a white solid (mp 59–60 °C): IR (Nujol) 3240 (NH), 1170 (C=S) cm^{-1}; ^1H NMR ($CDCl_3$) δ 0.89 (t, 3H, CH_3, $J = 7.5$ Hz), 1.57 (m, 2H, $CH_3CH_2CH_2$), 3.56 (t, 2H, $CH_3CH_2CH_2$, $J = 6.9$ Hz), 7.42–7.43 (m, 5H, arom); Anal. ($C_{10}H_{14}N_2S$) C, H, N.

6.3. Synthesis of 2-imino-4-thiazolidinones

A solution of chloroacetyl chloride (1.69 g, 0.015 mol) in chloroform (20 mL) was added dropwise to a stirred solution of **1** (1.94 g, 0.01 mmol) and triethylamine (2.02 g, 0.02 mol) in chloroform (30 mL) and the mixture was stirred overnight at room temperature. Removal of the solvent gives an oily residue, which was dissolved in ethyl ether and repeatedly washed with an aqueous sodium carbonate (10%). The organic layer was dried over sodium sulfate, filtered, and concentrated.

The crude mixture was purified by silica gel column chromatography (eluent petroleum ether/ethyl ether, 3/2) to give **2a** (0.73 g, 31%) and **2b** (1.45 g, 62%), each as a white solid.

6.3.1. 2-Phenylimino-3-propyl-4-thiazolidinone (2a). mp 56–58 °C; ^1H NMR ($CDCl_3$) δ 0.97 (t, 3H, CH_3, $J = 7.5$ Hz), 1.75 (m, 2H, $CH_3CH_2CH_2$), 3.80 (s, 2H, 5-CH_2), 3.82 (t, 2H, $CH_3CH_2CH_2$, $J = 7.5$ Hz), 6.97–7.36 (m, 5H, arom); ^{13}C NMR ($CDCl_3$) δ 11.1 (CH_3); 20.4 ($CH_3CH_2CH_2$); 32.5 (5-CH_2); 44.5 ($CH_3CH_2CH_2$);

154.0 (2-C); 120.7, 124.3, 129.0, 137.8 (CH arom); 171.6 (*C*O); Anal. ($C_{12}H_{14}N_2OS$) C, H, N.

6.3.2. 3-Phenyl-2-propylimino-4-thiazolidinone (2b). mp 146–148 °C; ^{1}H NMR ($CDCl_3$) δ 0.91 (t, 3H, CH_3, J = 7.5 Hz), 1.61 (m, 2H, $CH_3CH_2CH_2$), 3.27 (s, 2H, $CH_3CH_2CH_2$, J = 6.9 Hz), 3.97 (s, 2H, 5-CH_2), 7.27–7.52 (m, 5H, arom); ^{13}C NMR ($CDCl_3$) δ 12.9 (CH_3); 24,6 ($CH_3CH_2CH_2$); 33.7 (5-CH_2); 55.3 ($CH_3CH_2CH_2$); 152.8 (2-C); 129.0, 129.7 130.2, 136.2 (CH arom); 174.5 (*C*O); Anal. ($C_{12}H_{14}N_2OS$) C, H, N.

6.4. General procedures for the synthesis of 5-arylidene-2-phenylimino-3-propyl-4-thiazolidinones (3a, 4a, and 6a–8a)

To a solution of **2a** and/or **2b** compounds (0.7 g, 0.03 mol) and piperidine (0.35 g, 0.04 mol) in ethanol (35 mL) the appropriate benzaldehyde (0.03 mol) was added and the mixture was heated at reflux for 20–24 h. After this time, the solution was concentrated in vacuo and kept at −15 °C over 2 h. The residue was filtered off and recrystallized from methanol.

6.4.1. 5-(3-Methoxyphenyl)methylidene-2-phenylimino-3-propyl-4-thiazolidinone (3a). Yield 70%; mp 115–118 °C. ^{1}H NMR ($CDCl_3$) δ 1.02 (t, 3H, CH_3, J = 7.5 Hz); 1.84 (m, 2H, $CH_3CH_2CH_2$); 3.80 (s, 3H, OCH_3); 3.98 (t, 2H, $CH_3CH_2CH_2$, J = 7.2 Hz); 7.28–7.42 (m, 9H, arom); 7.71 (s, 1H, CH); ^{13}C NMR ($CDCl_3$) δ 11.2 (CH_3); 20.75 ($CH_3CH_2CH_2$); 44.7 ($CH_3CH_2CH_2$); 55.2 (O*C*H$_3$); 115.2, 115.4, 121.1, 122.0, 124.7, 129.3, 129.9 (CH arom); 118.9 (5-C); 130.4 (CH methylidene); 126.6, 148.4 (Cq arom); 166.6 (CO); Anal. ($C_{20}H_{20}N_2O_2S$) C, H, N.

6.4.2. 5-(4-Methylthiophenyl)methylidene-2-phenylimino-3-propyl-4-thiazolidinone (4a). Yield 84%; mp 130–132 °C. ^{1}H NMR ($CDCl_3$) δ 1.06 (t, 3H, CH_3, J = 7.4 Hz); 1.87 (m, 2H, $CH_3CH_2CH_2$); 2.52 (s, 3H, SCH_3); 4.04 (t, 2H, $CH_3CH_2CH_2$, J = 7.5 Hz); 7.06–7.47 (m, 9H, arom); 7.75 (s, 1H, CH); ^{13}C NMR ($CDCl_3$) δ 11.3 (CH_3); 15.0 (SCH_3); 20.8 ($CH_3CH_2CH_2$); 44.8 ($CH_3CH_2CH_2$); 120.5 (5-C); 121.2, 124.8, 125.8, 129.3, 130.1 (CH arom); 130.2 (CH methylidene) 141.6, 148.3, 150.5 (Cq arom); 166.9 (CO); Anal. ($C_{20}H_{20}N_2OS_2$) C, H, N.

6.4.3. 5-(4-Methoxyphenyl)methylidene-2-phenylimino-3-propyl-4-thiazolidinone (6a). Yield 81%; mp 106–108 °C. ^{1}H NMR ($CDCl_3$) δ 1.02 (t, 3H, CH_3, J = 7.2 Hz); 1.83 (m, 2H, $CH_3CH_2CH_2$); 3.83 (s, 3H, OCH_3); 3.97 (t, 2H, $CH_3CH_2CH_2$, J = 7.5 Hz); 6.94–7.40 (m, 9H, arom); 7.70 (s, 1H, CH); ^{13}C NMR ($CDCl_3$) δ 11.3 (CH_3); 20.8 ($CH_3CH_2CH_2$); 44.7 ($CH_3CH_2CH_2$); 55.3 (OCH_3); 114.6, 121.2, 124.6, 129.3, 130.4 (CH arom); 119.0 (5-C); 131.7 (CH methylidene); 126.5, 148.5, 150.7, 160.7 (Cq arom); 167.1 (CO); Anal. ($C_{20}H_{20}N_2O_2S$) C, H, N.

6.4.4. 5-(4-Chlorophenyl)methylidene-2-phenylimino-3-propyl-4-thiazolidinone (7a). Yield 79%; mp 134–136 °C. ^{1}H NMR ($CDCl_3$) δ 1.06 (t, 3H, CH_3, J = 7.2 Hz); 1.86 (m, 2H, $CH_3CH_2CH_2$); 4.03 (t, 2H, $CH_3CH_2CH_2$, J = 7.4 Hz); 7.07–7.45 (m, 9H, arom); 7.73 (s, 1H, CH); ^{13}C NMR ($CDCl_3$) δ 11.3 (CH_3); 20.8 ($CH_3CH_2CH_2$); 44.9 ($CH_3CH_2CH_2$); 121.1, 124.9, 129.1, 129.3, 129.4 (CH arom); 122.6 (5-C); 131.0 (CH methylidene); 132.4, 135.6, 148.2, 149.9 (Cq arom); 166.6 (CO); Anal. ($C_{19}H_{17}ClN_2OS$) C, H, N.

6.4.5. 5-(3,4-Dimethoxyphenyl)methylidene-2-phenylimino-3-propyl-4-thiazolidinone (8a). Yield 68%; mp 170–172 °C. ^{1}H NMR ($CDCl_3$) δ 1.08 (t, 3H, CH_3, J = 7.2 Hz); 1.83 (m, 2H, $CH_3CH_2CH_2$); 3.94 (t, 2H, $CH_3CH_2CH_2$, J = 7.5 Hz); 3.96, 3.99 (2s, 6H, OCH_3); 7.08–7.63 (m, 8H, arom); 7.80 (s, 1H, CH); ^{13}C NMR ($CDCl_3$) δ 11.2 (CH_3); 20.8 ($CH_3CH_2CH_2$); 44.8 ($CH_3CH_2CH_2$); 55.9, 56.0 (OCH_3); 111.4, 113.2, 121.3, 123.4, 124.9, 130.9 (CH arom); 119.2 (5-C); 129.3 (CH methylidene); 119.2, 126.8, 149.2, 150.6 (Cq arom); 166.9 (CO); Anal. ($C_{21}H_{22}N_2O_3S$) C, H, N.

6.5. Synthesis of 5-(4-methylsulfonylphenyl)methylidene-2-phenylimino-3-propyl-4-thiazolidinone (5a)

A solution of **4a** (0.5 g, 0.2 mol) in 30 mL acetic acid (50%) was treated dropwise with 30 g (0.3 mol) H_2O_2 (35%) and stirred for 3 h at reflux. The mixture was then added to water (40 mL) and cooled for 24 h on ice, before being filtered-off. Yield 78%; mp 127–128 °C. ^{1}H NMR ($CDCl_3$) δ 1.04 (t, 3H, CH_3, J = 7.5 Hz); 1.85 (m, 2H, $CH_3CH_2CH_2$); 3.06 (s, 3H, SO_2CH_3); 4.04 (t, 2H, $CH_3CH_2CH_2$, J = 7.5 Hz); 7.96–7.63 (m, 9H, arom); 7.70 (s, 1H, CH); ^{13}C NMR ($CDCl_3$) δ 11.3 (CH_3); 15.0 (SO_2CH_3); 20.8 ($CH_3CH_2CH_2$); 44.8 ($CH_3CH_2CH_2$); 120.6 (5-C); 121.3, 124.9, 126.0, 129.4, 130.2 (CH arom); 130.3 (CH methylidene); 141.7, 148.2, 150.7 (Cq arom); 166.9 (CO); Anal. ($C_{20}H_{20}N_2O_3S_2$) C, H, N.

7. Pharmacology

7.1. Assessment of COX-1/COX-2 activity

7.1.1. Compounds tested. Stock solutions of test compounds were prepared in ethanol; an equivalent amount of ethanol was included in control samples.

7.1.2. Cell culture. The murine monocyte/macrophage J774 cell line was grown in Dulbecco's modified Eagles medium (DMEM) supplemented with 2 mM glutamine, 25 mM Hepes, penicillin (100 U/mL), streptomycin (100 μg/mL), 10% fetal bovine serum (FBS), and 1.2% Na pyruvate (Bio Whittaker, Europe). Cells were plated in 24-well culture plates at a density of 2.5×10^5 cells/mL or in 10 cm-diameter culture dishes (1×10^7 cells/10 mL/dish) and allowed to adhere at 37 °C in 5% CO_2 and 95% O_2 for 2 h. Immediately before the experiments, culture medium was replaced by fresh medium without FBS in order to avoid interference with radioimmunoassay[11] and cells were stimulated as described.

7.1.3. Assessment of COX-1 activity. The in vitro screening scheme included COX-1 activation by stimulation of

cells with arachidonic acid (15 μM) for 30 min inducing a significant increase of PGE_2 (3.5 ± 0.09 ng/10^6 cells) in comparison to unstimulated cells (0.35 ± 0.07 ng/10^6 cells).

Cells were pretreated with test compounds for 15 min and further incubated for 30 min with arachidonic acid (15 μM).[11] At the end of the incubation the supernatants were collected for the measurement of PGE_2 by radioimmunoassay.[21] All compounds were assayed at three concentrations (0.1, 1, and 10 μM).

7.1.4. Assessment of COX-2 activity. Cells were stimulated, for 24 h, with *Escherichia coli* lipopolysaccharide (LPS, 10 μg/mL), to induce COX-2. The supernatant of the cells was replaced with fresh medium, cells pretreated with test compounds, at the concentrations previously reported, for 15 min and further incubated for 30 min with arachidonic acid. There was a marked increase in PGE_2 production from 2.07 ± 0.04 to 27.2 ± 2.8 ng/10^6 cells ($p < 0.001$). At the end of the incubation the supernatants were collected for the measurement of PGE_2 by radioimmunoassay.

7.2. Anti-inflammatory activity

7.2.1. Animals. Male Sprague–Dawley rats (300–350 g; Charles River, Milan, Italy) were housed in a controlled environment and provided with standard rodent chow and water. Animal care was in compliance with Italian regulations on protection of animals used for experimental and other scientific purposes (D.M. 116192) as well as with the EEC regulations (O.J. of E.C. L 358/1 12/18/1986).

7.2.2. Carrageenan-induced paw edema. Rats received a subplantar injection of 0.2 mL saline containing 2% λ-carrageenan in the right hindpaw. A suspension of tested compounds (10 mg/kg), or an equivalent volume of vehicle (DMSO 50%), were administered intraperitoneally 30 min before carrageenan. Control animals received the same volume of vehicle. The volume of the paw was measured by plethysmometry (model 7140, Ugo Basile) immediately after the injection. Subsequent readings of the volume of the same paw were carried out at 60-min intervals and compared to the initial readings.

7.2.3. Carrageenan-induced pleurisy. Rats were anaesthetized with isoflurane and submitted to a skin incision at the level of the left sixth intercostal space. The underlying muscle was dissected and saline (0.2 mL) or saline containing 2% λ-carrageenan (0.2 mL) was injected into the pleural cavity. The skin incision was closed with a suture and the animals allowed to recover. A suspension of tested compounds (20 mg/kg), or an equivalent volume (0.6 mL) of vehicle (DMSO 50%), were administered intraperitoneally 30 min before carrageenan. At 4 h after the injection of carrageenan, the animals were killed by inhalation of CO_2. The chest was carefully opened and the pleural cavity rinsed with 2 mL of saline solution containing heparin (5 U/mL) and indomethacin (10 μg/mL). The exudate and washing solution were removed by aspiration and the total volume measured. Any exudate that was contaminated with blood was discarded. The amount of exudate was calculated by subtracting the volume injected (2 mL) from the total volume recovered. The leukocytes in the exudate were suspended in phosphate-buffer saline (PBS) and counted with an optical microscope in a Burker's chamber after Trypan Blue staining.

7.2.4. Measurement of prostaglandin E_2 in the pleural exudate. The amount of prostaglandin E_2 (PGE_2) present in the pleural fluid was measured by radioimmunoassay without prior extraction or purification.[21]

7.2.5. Myeloperoxidase activity. Myeloperoxidase (MPO) activity, an indicator of polymorphonuclear leukocyte (PMN) accumulation, was determined as previously described.[22] At the specified time following injection of carrageenan, lung tissues were obtained and weighed and each piece homogenized in a solution containing 0.5% (w/v) hexadecyltrimethyl-ammonium bromide dissolved in 10 mM potassium phosphate buffer (pH 7) and centrifuged for 30 min at 20,000*g* at 4 °C. An aliquot of the supernatant was then allowed to react with a solution of tetramethylbenzidine (1.6 mM) and 0.1 mM hydrogen peroxide. The rate of change in absorbance was measured spectrophotometrically at 650 nm. MPO activity was defined as the quantity of enzyme degrading 1 μmol of peroxide/min at 37 °C and was expressed in U 100 mg^{-1} of wet tissue.

7.2.6. Materials. Arachidonic acid was obtained from SPIBIO, Paris, France. [^{3}H-PGE_2] was from NEN Du Pont (Milan, Italy). Bacterial lipopolysaccharide from *Salmonella thyphosa* (LPS) and all other reagents and compounds used were obtained from Sigma–Aldrich, Milan, Italy.

7.2.7. Data analysis. All values in the figures and text are expressed as means ± standard error of the mean (SEM) for *n* observations. For the in vitro studies, the data represent the number of wells studied (6 to 9 wells from 2 to 3 independent experiments). For the in vivo studies, *n* represents the number of animals studied. The results were analyzed by one-way analysis of variance (ANOVA) followed by a Bonferroni post-hoc test for multiple comparisons. A *p* value less than 0.05 was considered significant. In the experiments involving histology, the figures shown are representative of at least three experiments performed on different experimental days.

7.3. Computational studies

7.3.1. Structures. (1) *Protein*: The X-ray structure of COX-2 complexed with the inhibitor SC-558 was retrieved from the Brookhaven Protein Data Bank (entry code 6COX)[14] and used as target for our modeling studies. Since the positions of most water molecules in the crystal structure complex are unlikely to be conserved, water molecules were excluded before the docking protocols. Residues with missing side chain atoms were rebuilt using the Biopolymer module integrated into Insight II.[19] Using the AutoDockTools package,[18] non-polar hydrogen atoms were added to the protein,

lone pairs were merged, Kollman united-atom partial charges were assigned and finally solvent parameters were enclosed.

(2) *Ligands*: Coordinates for SC-558 were taken directly from the X-ray structure of its complex with COX-2. The structure of **6a** was constructed using standard bond lengths and angles from the Sybyl fragment library and fully optimized by semiempirical quantum mechanical method AM1.[23] The AutoDockTools was used to identify the aromatic carbons, assign the rigid root, and the active torsions.

7.3.2. Docking calculations. Docking studies to COX-2 were carried out using the package AutoDock 3.0, a program that allows torsional flexibility in the ligand, while the protein is kept rigid.[18] The grid spacing was 0.375 Å in each dimension, and each grid map consists of $60 \times 60 \times 60$ grid points. The grid was centered on the selective site, using the SC-558 crystallographic position as reference. The AutoGrid program generated separate grid maps for all atom types of the ligand structures plus one for electrostatic interactions. We used the so-called Lamarckian genetic algorithm (LGA), which combines a traditional genetic algorithm (GA) with a local search method. For both ligands, each LCG job consists of 100 independent runs, starting each time from a different position and orientation chosen randomly. The binding modes were clustered using rmsd cutoff of 1.0 Å with respect to the starting position. All the other values were used as default settings and the results were ranked by the lowest energy representative of each cluster combined with the root mean square deviation.

Acknowledgment

This work was financially supported by the Fondo Ateneo di Ricerca (University of Messina, Italy).

References and notes

1. Bombardier, C.; Laine, L.; Reicin, A.; Shapiro, D.; Burgos-Vargas, R.; Davis, B.; Day, R.; Bosi Ferraz, M.; Hawkey, C. J.; Hochberg, M. C.; Kvien, T. K.; Schnitzer, T. J. *N. Eng. J. Med.* **2000**, *343*, 1520.
2. Silverstein, F. E.; Faich, G.; Goldstein, J. L.; Simon, L. S.; Pincus, T.; Whelton, A.; Makuch, R.; Eisen, G.; Agrawal, N. M.; Stenson, W. F.; Burr, A. M.; Zhao, W. W.; Kent, J. D.; Lefkowith, J. B.; Verburg, K. M.; Geis, G. S. *JAMA* **2000**, *284*, 1247.
3. Vane, J.; Botting, R. *FASEB J.* **1987**, *1*, 89–96.
4. Smith, W. L.; Dewitt, D. L. *Adv. Immunol.* **1996**, *62*, 167–215.
5. Fu, J. Y.; Masferrer, J. L.; Seibert, K.; Raz, A.; Needleman, P. *J. Biol. Chem.* **1990**, *265*, 16737–16740.
6. Herschman, H. R. *Biochim. Biophys. Acta* **1996**, *1299*, 125–140.
7. Dubois, R. N.; Abramson, S. B.; Crofford, L.; Gupta, R. A.; Simon, L. S.; Van De Putte, L. B.; Lipsky, P. E. *FASEB J.* **1998**, *12*, 1063–1073.
8. De Leval, X.; Delarge, J.; Somers, F.; De Tullio, P.; Henrotin, Y.; Pirotte, B.; Dogne, J. M. *Curr. Med. Chem.* **2000**, *7*, 1041–1062.
9. Celecoxib *Drugs Future* **1997**, *22*, 711–714.
10. (a) Previtera, T.; Vigorita, M. G.; Basile, M.; Fenech, G.; Trovato, A.; Occhiuto, F.; Monforte, M. T.; Barbera, R. *Eur. J. Med. Chem.* **1990**, *25*, 569–579; (b) Vigorita, M. G.; Previtera, T.; Basile, M.; Fenech, G.; Costa De Pasquale, R.; Occhiuto, F.; Circosta, C. *Il Farmaco* **1988**, *4*, 373–379; (c) Vigorita, M. G.; Previtera, T.; Ottanà, R.; Grillone, I.; Monforte, F.; Monforte, M. T.; Trovato, A.; Rossitto, A. *Il Farmaco* **1997**, *52*, 43–48; (d) Vigorita, M. G.; Ottanà, R.; Monforte, F.; Maccari, R.; Monforte, M. T.; Trovato, A.; Taviano, M. F.; Miceli, N.; De Luca, G.; Alcaro, S.; Ortuso, F. *Bioorg. Med. Chem.* **2003**, *11*, 999–1006; (e) Ottanà, R.; Mazzon, E.; Dugo, L.; Monforte, F.; Maccari, R.; Sautebin, L.; De Luca, G.; Vigorita, M. G.; Alcaro, S.; Ortuso, F.; Caputi, A. P.; Cuzzocrea, S. *Eur. J. Pharmacol.* **2002**, *448*, 71–80.
11. Di Rosa, M.; Willoughby, D. A. *J. Pharm. Pharmacol.* **1971**, *23*, 297–298.
12. Cuzzocrea, S.; Zingarelli, B.; Gilard, E.; Hake, P.; Salzman, A. L.; Szabò, C. *Free Radical Biol. Med.* **1998**, *24*, 450–459.
13. Zingarelli, B.; Southan, G. J.; Gilad, E.; O'Connor, M.; Salzman, A. L.; Szabo, C. *Br. J. Pharmacol.* **1997**, *120*, 357–366.
14. Kurumbail, R. G.; Stevens, A. M.; Gierse, J. K.; McDonald, J. J.; Stegeman, R. A.; Pak, J. Y.; Gildehaus, D.; Miyashiro, J. M.; Penning, T. D.; Seibert, K.; Isakson, P. C.; Stallings, W. C. *Nature* **1996**, *384*, 644–648.
15. (a) Momose, Y.; Meguro, K.; Ikeda, H.; Hatanaka, C.; Oi, S.; Sohda, T. *Chem. Pharm. Bull.* **1991**, *39*, 1440–1445; (b) Ispida, T.; In, Y.; Inoue, M.; Tanaka, C.; Hamanaka, N. *J. Chem. Soc., Perkin Trans.* **1990**, 1085–1091.
16. Bruno, G.; Costantino, L.; Curinga, C.; Maccari, R.; Monforte, F.; Nicolò, F.; Ottanà, R.; Vigorita, M. G. *Bioorg. Med. Chem.* **2002**, *10*, 1077–1084.
17. Abdel-Salam, O. M. E.; Baiuomy, A. R.; Arbid, M. S. *Pharm. Res.* **2004**, *49*, 119.
18. Morris, G. M.; Goodsell, D. S.; Halliday, R. S.; Huey, R.; Hart, W. E.; Belew, R. K.; Olson, A. J. *J. Comput. Chem.* **1998**, *19*, 1639–1662.
19. InsightII 2000. Accelrys, Inc., San Diego, CA, http://www.accelrys.com.
20. Gierse, J. K.; Mc Donald, J. J.; Hauser, S. D.; Rangwala, S. H.; Kobolt, C. M.; Seibert, K. *J. Biol. Chem.* **1996**, *271*, 15810–15814, and references cited therein.
21. Sautebin, L.; Ialenti, A.; Ianaro, A.; Di Rosa, M. *Br. J. Pharmacol.* **1995**, *114*, 323–328.
22. Mullane, K. M.; Westlin, W.; Kraemer, R. *Ann. N.Y. Acad. Sci.* **1988**, *524*, 103–113.
23. SYBYL 6.9. Tripos Associates Inc., St. Louis, Missouri, USA.
24. DeLano, W. L. The PyMol Molecular Graphics System (2002) on World Wide Web http://www.pymol.org.